

Effect of Different Near-Wall Treatments on Indoor Airflow Simulations

N. El Gharbi^{1,3}, R. Absi^{2†}, A. Benzaoui³

¹ Center for Renewable Energy Development, Po. Box 62 Bouzareah 16340 Algiers, Algeria

² EBI, Inst. Polytech. St-Louis, PRES UPGO – Université Paris Grand Ouest, 32 Boulevard du Port, 95094, Cergy-Pontoise Cedex, France

³ University of Sciences and Technology Houari Boumediene (USTHB), Po. Box 32 El Alia Bab Ezzouar 16111 Algiers, Algeria

†Corresponding Author Email: rafik.absi@yahoo.fr

(Received October 30, 2010; accepted July 4, 2011)

ABSTRACT

Airflow simulation results depend on a good prediction of near wall turbulence. In this paper a comparative study between different near wall treatments is presented. It is applied to two test cases in building: (1) the first concerns flow through a long corridor which is similar to that in a fully developed plane channel. Simulation results are compared to direct numerical simulation (DNS) data of Moser *et al.* (1999) for $Re_\tau = 590$ (where Re_τ denotes the friction Reynolds number defined by friction velocity u_τ , kinematics viscosity ν and the channel half-width δ); (2) the second case is a benchmark test for room air distribution. Simulation results are compared to experimental data obtained with laser-Doppler anemometry (Nielsen, 1990). Simulations were performed with the aid of CFD code Fluent (2005). Near wall treatments available in Fluent were tested: Standard Wall Functions, Non Equilibrium Wall Function and Enhanced Wall Treatment. In each case, suitable meshes with adequate position of the first near-wall node are needed. Results of near-wall mean stream wise velocity u^+ and turbulent kinetic energy k^+ profiles are presented, variables with the superscript of + are those non dimensional by the wall friction velocity u_τ and the kinematic viscosity ν .

Keywords: CFD, Airflow, Turbulence, Simulation, Near-Wall treatment, Channel, Room.

NOMENCLATURE

C_1, C_2	Constant of empirical turbulence model for $k-\varepsilon$ one
G_k	Generation of k , (Nm^{-2})
H	High, (m)
k	Turbulent kinetic energy, ($\text{m}^2 \text{s}^{-2}$)
L	Width, (m)
R_{ij}	Reynolds stress tensor, ($\text{kg m}^{-1} \text{s}^{-2}$)
Re_τ	Friction Reynolds number
u_0	Inlet velocity, (m s^{-1})
u'_i, u'_j	Arbitrary fluctuating velocity component, (m s^{-1})
u_τ	Friction velocity, (m s^{-1})
x	Axial coordinate, (m)
x_i, x_j	Arbitrary direction, (m)
u_τ	Friction velocity, (m s^{-1})
y	Radial coordinate, (m)
y^+	No-dimensional wall coordinate

Greek symbols

δ_{ij}	Kronecker delta
ε	Turbulent energy dissipation rate, ($\text{m}^2 \text{s}^{-3}$)
μ	Dynamic viscosity, ($\text{kgm}^{-1} \text{s}^{-1}$)
μ_t	Turbulent viscosity, ($\text{kgm}^{-1} \text{s}^{-1}$)
ν	Kinematics viscosity, ($\text{m}^2 \text{s}^{-1}$)
ρ	Fluid density, (kgm^{-3})
τ_{ij}	Turbulent stress tensor, ($\text{m}^2 \text{s}^{-2}$)
τ_w	Wall shear stress, ($\text{kg m}^{-1} \text{s}^{-2}$)

Abbreviation

CFD	Computational Fluid Dynamics
DNS	Direct Numerical Simulation
EWT	Enhanced Wall Treatment
NEWF	Non-Equilibrium Wall Function
RMS	Root Mean Square
SWF	Standard Wall Function
TKE	Turbulent Kinetic Energy

1. INTRODUCTION

Most people spend the majority of their time indoors, often in shared spaces, so the expectations of the occupant for a thermally comfortable indoor climate have risen. For this reason tools are required to determine and predict the flow characteristics in the early design phase. The CFD method is often employed.

For predicting room air flow, the standard $k-\varepsilon$ turbulence model has enjoyed the greatest usage (Murakami *et al.* (1987), Nielsen (1989), Chen *et al.* (1992), Weathers (1992), Haghghat *et al.* (1992), Chen (1995), El Gharbi (2007), Sumon *et al.* (2008), Bahlaoui *et al.* (2011), El Gharbi *et al.* (2012)). However this model is only valid for fully-developed turbulence, the flow is not solved up the wall. In addition, the wall is the most common boundary encountered in these confined fluid flow problems. Therefore, to simulate this region the selection of appropriate near-wall treatment methods is very important for obtaining reliable prediction results of airflows simulation. The first near wall treatments was developed with $k-\varepsilon$ model, we quoted: Spalding (1961), Wolfstein (1969), Launder *et al.* (1974), Chen *et al.* (1988), Jongen (1992), Kim *et al.* (1995).

This investigation studied two typical indoor airflows: (1) a flow in a fully developed plane channel, assimilated to flow through a long corridor, (2) a forced convection flow in a ventilated room, a benchmark test for 2D room air distribution. Fluid flow near a solid wall as well as the characteristics of turbulent flow near such structures is considered. Simulations will be performed with the aid of the commercial CFD code Fluent (2005). All different near wall treatments available in Fluent will be tested: Standard Wall Functions, Non Equilibrium Wall Function and Enhanced Wall Treatment. We will investigate both effects of meshes and position of the first near-wall node.

For the first test case simulations results are compared to direct numerical simulation (DNS) data of Moser *et al.* (1999) for $Re_\tau = 590$ (where Re_τ denotes the friction Reynolds number defined by friction velocity u_τ , kinematic viscosity ν and the channel half-width δ). Then, for the second test case, the simulation results are compared with experimental data obtained with laser-Doppler anemometry (Nielsen, 1990). This one is use to measure velocity and velocity fluctuation.

1. MODEL EQUATIONS

A. Governing Equations

In this study, airflow is modeled using the standard $k-\varepsilon$ model. The governing equations are:

Mass conservative equation:

$$\frac{\delta(\rho u_i)}{\delta x_i} = 0 \quad (1)$$

Momentum conservation equation:

$$\frac{\delta(\rho u_i v_j)}{\delta x_i} = -\frac{\delta p}{\delta x_i} + \frac{\delta \tau_{ij}}{\delta x_j} + \frac{\delta R_{ij}}{\delta x_j} \quad (2)$$

where τ_{ij} is the viscous stress tensor and R_{ij} is the turbulent Reynolds stress tensor

$$\tau_{ij} = \mu \left(\frac{\delta u_i}{\delta x_j} + \frac{\delta u_j}{\delta x_i} \right) - \frac{2}{3} \mu \left(\frac{\delta u_k}{\delta x_k} \right) \delta_{ij} \quad (3)$$

$$R_{ij} = -\overline{\rho u_i u_j} = \mu_t \left(\frac{\delta u_i}{\delta x_j} + \frac{\delta u_j}{\delta x_i} \right) - \frac{2}{3} \rho k \delta_{ij} \quad (4)$$

Turbulent kinetic energy:

$$\rho u_i \frac{\delta k}{\delta x_i} = \frac{\delta}{\delta x_i} \left[\left(\mu + \frac{\mu_t}{\sigma_k} \right) \frac{\delta k}{\delta x_i} \right] + G_k - \rho \varepsilon \quad (5)$$

Dissipation rate:

$$\rho u_i \frac{\delta \varepsilon}{\delta x_i} = \frac{\delta}{\delta x_i} \left[\left(\mu + \frac{\mu_t}{\sigma_\varepsilon} \right) \frac{\delta \varepsilon}{\delta x_i} \right] + C_1 \left(\frac{\varepsilon}{k} \right) G_k - C_2 \rho \frac{\varepsilon^2}{k} \quad (6)$$

$$\mu_t = C_\mu \rho \left(\frac{k^2}{\varepsilon} \right) \quad (7)$$

$$G_k = \mu_t \left(\frac{\delta u_i}{\delta x_j} + \frac{\delta u_j}{\delta x_i} \right) \frac{\delta u_j}{\delta x_i} - \frac{2}{3} \rho k \delta_{ij} \frac{\delta u_j}{\delta x_i} \quad (8)$$

B. Near-wall Treatments

Close to the wall, the flow is influenced by viscous effects. The mean velocity field is affected through the no-slip condition that has to be satisfied at the wall. Toward the outer part of the near-wall region, however, the turbulence is rapidly augmented by the production of turbulence kinetic energy due to the large gradients in mean velocity.

Therefore, accurate representation of the flow in the near-wall region determines successful predictions of wall-bounded turbulent flows. For that and because most $k-\varepsilon$ and RSM turbulence models will not predict correct near-wall behavior if integrated down to the wall, special near-wall treatment is required.

Fluent near-wall treatments:

Fluent offers two approaches based on the classical theory describing the flow near-walls in turbulent flows, Fluent (2005), Fig. 1:

- a. The first one is a semi-empirical approach, and uses the so called "wall function" to bridge the viscosity affected region between the wall and the fully turbulent region. The viscous sublayer and buffer layer region are not resolved. Therefore, the near-wall mesh may be relatively coarse, the first grid point off the wall must be positioned in the log law region at $y^+ > 30$ (the distance being measured in wall units $y^+ = y u_\tau / \nu$, where u_τ is the friction velocity). This approach is justified for

industrial flows with high Reynolds numbers, because it saves computational time and it is sufficiently precise. There are two options for semi-empirical approach use in Fluent code. The first “Standard Wall Function” (Launder *et al.* 1974) is presented as default in Fluent. It assumes equilibrium between the production and dissipation of turbulent kinetic energy. The second “Non-Equilibrium Wall Function” (Kim *et al.* 1995) may be selected by the user. It does not assume this equilibrium, but allows differing production and dissipation, as may be the case for flows where there is separation and reattachment or severe pressure gradients (Fluent 2005).

- b. The second approach combines a two layer model (where the viscosity affected near-wall region is completely resolved, along the way to the viscous sublayer), together with enhanced wall functions. Generally, it requires a very fine near-wall mesh. The first grid point off the wall must be from $y^+ \approx 1$. This approach is more suited for low-Reynolds number flows with complex near-wall phenomena. Although it obviously requires a greater amount of computational resources. (Fluent 2005).

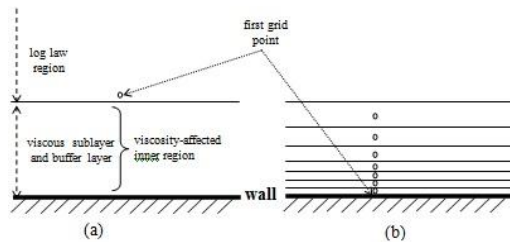


Fig. 1. Schematics of (a), the wall function approach and (b) the two-layer approach

2. TEST CASES

Airflow simulations with different near-wall treatments are applied to two test cases:

A. Channel flow

The first test case is the plane fully developed channel flow similar to flow through a long corridor in a building, Fig. 2. Simulations results are validated by DNS data of Moser *et al.* (1999) for $Re_\tau = 590$.

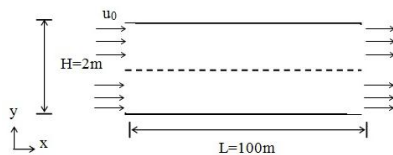


Fig. 2. Presentation of the channel flow

B. Room air distribution

The second test case is a benchmark test (Annex 20, Nielsen, 1990) for a room air distribution, Fig. 3. The simulation results are validated by experimental data obtained with Laser-Doppler Anemometry.

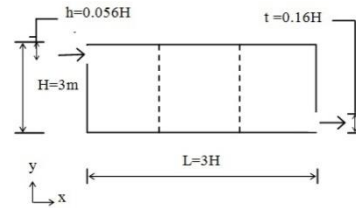


Fig. 3. Presentation of Nielsen's room, H=3m and L=9m.

3. RESULTS AND DISCUSSIONS

A. Effect of Mesh and First Grid Point

To captures boundary layer properly, the mesh should be correctly generated. For turbulent flows, calculation of the y^+ value of the first node point helps in doing that. This dimensionless distance is defined as:

$$y^+ = \frac{u_\tau y}{\nu} \quad (9)$$

where u_τ is the friction velocity defined as $\sqrt{\frac{\tau_w}{\rho}}$ and τ_w is the wall shear stress.

For that and because the wall distance y^+ is involved in the selection of the appropriate near-wall treatment, we do a grid test for only mesh in y direction. The geometry of a fully developed plane channel is chosen (first test case) and eight different mesh sizes are applied to select the appropriate mesh size that adapt with near-wall treatment (wall functions or near-wall modeling). This is achieved by refining the mesh, with particular attention to the first grid point off the wall. Table 1 shows selected computational mesh and the corresponding wall y^+ values.

Table 1 Different mesh

	mesh size (x×y)	first y^+	mesh type
mesh 1	(500×10)	59	regular
mesh 2	(500×14)	42.142874	regular
mesh 3	(500×19)	31.052644	regular
mesh 4	(500×28)	21.071437	regular
mesh 5	(500×57)	10.350901	regular
mesh 6	(500×76)	7.763161	regular
mesh 7	(500×57)	1.3467045	exponential law
mesh 8	(500×76)	1.0026873	exponential law

Non-dimensional mean stream wise velocity profiles scaled by the wall velocity $u^+ = \frac{u}{u_\tau}$ and non-dimensional profiles of turbulent kinetic energy $k^+ = \frac{k}{u_\tau^2}$ are plotted (Figs. 4 and 5).

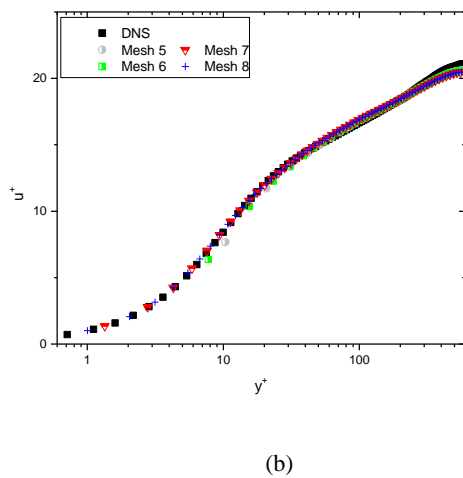
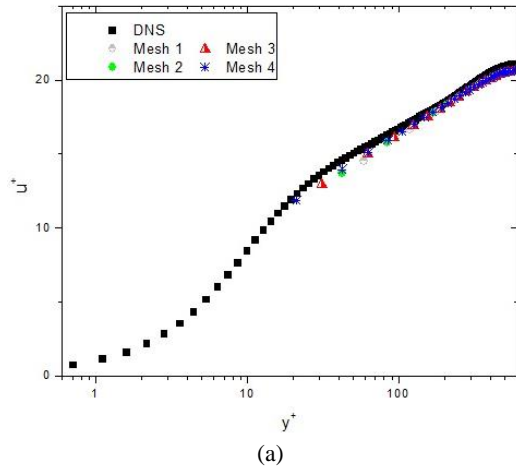


Fig.4. Comparison of non-dimensional mean streamwise velocity profiles using (a) coarse mesh with wall function (SWF), (b) fine mesh with near-wall modeling (EWT)

The different mesh configurations and corresponding wall y^+ value have significant influence on the computed non-dimensional mean streamwise velocity and turbulent kinetic energy profiles.

With wall functions, the first grid point must be in the log-law region i.e. $y^+ > 30$. **Figures 4(a) and 5(a)** show that mesh 3 seems to be the most appropriate. As a test case, **Fig. (6)** presents turbulent kinetic energy (TKE) and mean velocity profiles obtained by standard wall function and first grid point at $y^+ < 30$ ($y^+ \approx 10$ for mesh 5 and $y^+ \approx 1$ for mesh 7). It shows clearly that it is impossible to obtain correct predictions when we use fine mesh with wall functions. As illustrate in Figure 6, the distribution of u^+ and k^+ are significantly affected. Because wall functions use the assumption of local equilibrium, that is not valid in the viscosity affected region i.e. $y^+ < 30$.

With near wall modeling the first grid point must be in viscous sublayer i.e. $y^+ \approx 1$. **Figures 4(b) and 5(b)** show that mesh 7 seems to be the most appropriate. The viscosity affected near-wall region is completely resolved. According to user's guide of fluent (**Fluent, 2005**), with this modeling, we should have at least 10 cells within the viscosity affected near-wall region to be

able to resolve the mean velocity and turbulent quantities in that region.

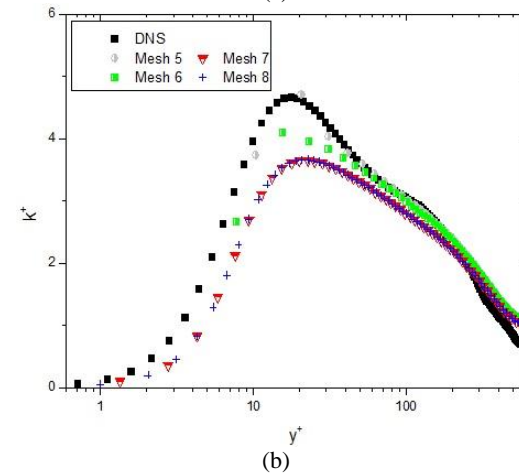
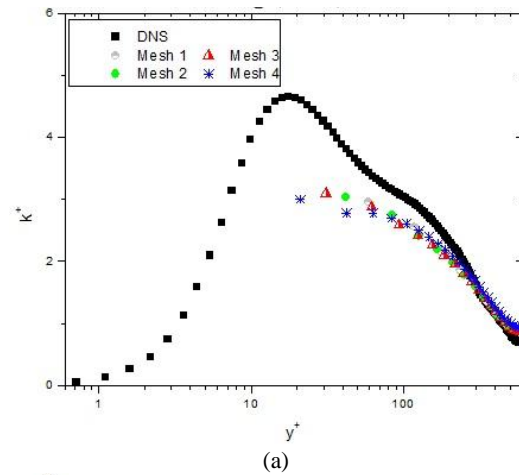


Fig. 5. Comparison of non-dimensional turbulent kinetic energy profiles using (a) coarse mesh with wall function (SWF), (b) fine mesh with near-wall modeling (EWT).

B. Selection of more appropriate near wall treatment

All different near wall treatments available in Fluent were tested: Standard wall function “SWF”, Non equilibrium wall function “NEWF” and Enhanced wall treatment “EWT”.

Results of mean streamwise velocity u^+ and turbulent kinetic energy k^+ profiles are presented in **Figs. (7) and (8)**.

For the two test cases, channel flow and room air distribution, a fine mesh (respectively 500×57 and 45×38) was used for enhanced wall treatment “EWT”, while a coarse mesh (respectively 500×19 and 45×12) was used for standard wall function “SWF” and non-equilibrium wall function “NEWF”.

For the first test case (plane channel flow), **Fig. 7** presents simulation results: mean streamwise velocity u^+ (**Fig. 7(a)**) and TKE k^+ (**Fig. 7(b)**) profiles, with DNS data of **Moser *et al.* (1999)** for $Re_\tau = 590$.

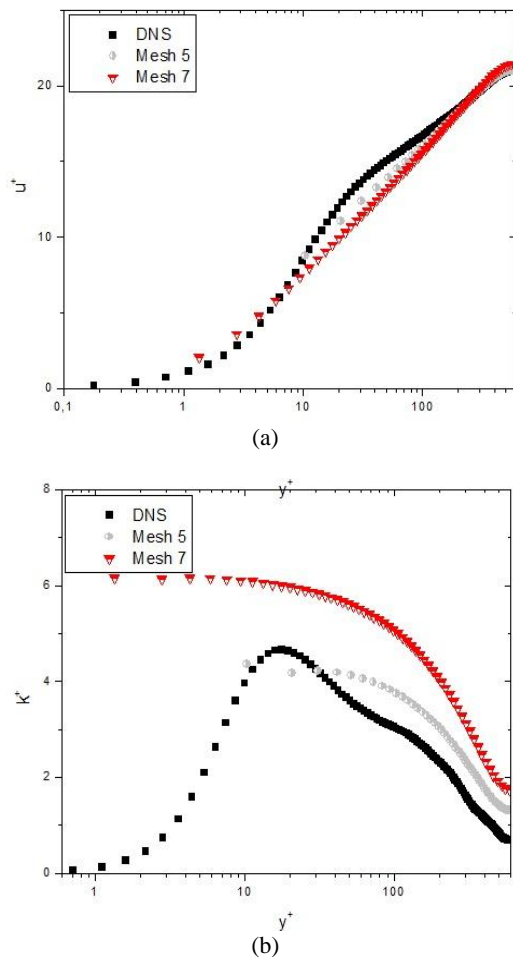


Fig. 6. Standard wall function using fine mesh
(a) non-dimensional mean stream wise velocity profiles
(b) non-dimensional turbulent kinetic energy profiles

On the one hand, standard “SWF” and non equilibrium “NEWF” wall functions need a coarse mesh (Fig. 1.a). The first node should be at $y^+ > 30$. Figure (7) shows that standard “SWF” and Non equilibrium “NEWF” wall functions predict well velocity profiles for $y^+ > 30$ and TKE profiles for $y^+ > 60$.

However, these near wall treatments are not able to provide details about velocity and TKE in the viscous and buffer layers. If these treatments are used, it is possible to provide an accurate description of TKE by an analytical equation and velocity by solving an ordinary differential equation “ODE” (Absi, 2009). These treatments could be therefore associated to this simple and efficient analytical method.

On the other hand, enhanced wall treatment “EWT” needs a finest mesh in the viscous sublayer (Fig. 1(b)).

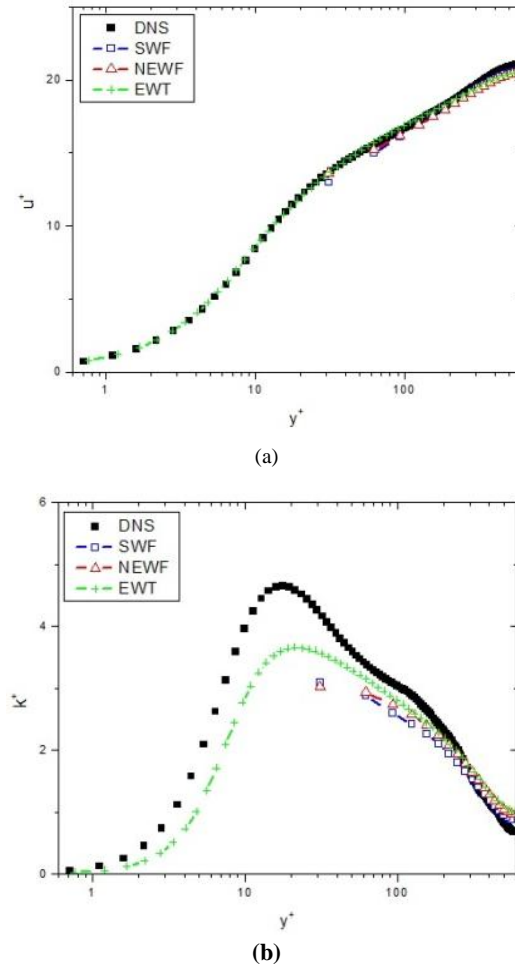


Fig. 7. comparison between predicted profiles using standard $k-\epsilon$ model with different wall treatments and DNS data for test case 1 plane channel flow. (a) mean streamwise velocity, (b) turbulent kinetic energy

The first node should be at about $y^+ \approx 1$. Figure (7) shows that the velocity profile is more accurate and well predicted even in the viscous and buffer layers than that standard “SWF” and non equilibrium “NEWF” wall functions. However, TKE is underestimated (Fig. 7(b)). This has no effect on velocity profile but can provide an underestimated eddy viscosity/diffusivity which could be involved in predicted particles concentrations.

In order to investigate the effect of standard $k-\epsilon$ model on the TKE profile which is underestimated by “EWT” (Fig. 7.b), a comparison with an advanced RANS models; Re-Normalisation Group “RNG” $k-\epsilon$ model (Yakhot *et al.* 1992), is done.

Figure (8) shows that RNG $k-\epsilon$ model provides a very small improvement for velocity and TKE. Since the difference is negligible, the underestimation of TKE seems therefore not related to the used turbulence model but associated to the near wall treatment.

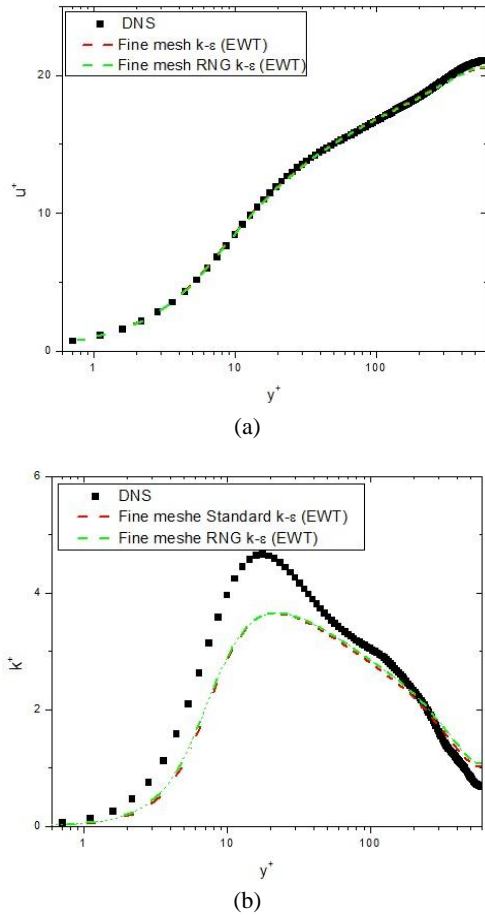


Fig. 8. Comparison between predicted profiles using standard and RNG $k-\epsilon$ models with enhanced wall treatment “EWT” and DNS data for test case 1 plane channel flow. (a) mean streamwise velocity, (b) turbulent kinetic energy

The second test case (benchmark test for a room air distribution), presents simulation results: mean velocity u^+ (Fig. 9(a) and 9(c)) and turbulence intensity (Fig. 9(b) and 9(d)), with experimental data obtained by laser-Doppler anemometry (Nielsen, 1990).

Figures 9(a) and 9(c) present mean velocity u^+ respectively at $x=3m$ ($1/3 L$) and $x=6m$ ($2/3 L$) while Figs. 9(b) and 8(d) present turbulence intensity u' respectively at $x=3m$ and $x=6m$. Figures (9) show that for $0 < y/H < 0.2$ and $0.8 < y/H < 1$, wall functions (“SWF” and “NEWF”) didn’t provide values, only “EWT” provides results. This is due to the required mesh and first near wall node.

Predicted mean velocity profiles with the different near-wall treatments are quite similar (Figs. 9(a), 9(c)) for $0.2 < y/H < 0.8$. However, “EWT” provides velocities near the walls (where wall functions are unable to provide values) but needs more computation time.

More important scatter is shown for RMS fluctuation velocities at $x=3m$ (Fig. 9(b)). All near-wall treatments fail to predict RMS fluctuation velocities for $0.2 < y/H < 0.5$. NEWF seems to be the less accurate. In contrast, at $x=6m$ (Fig. 9(d)) wall functions seem more accurate for $0.6 < y/H < 0.8$.

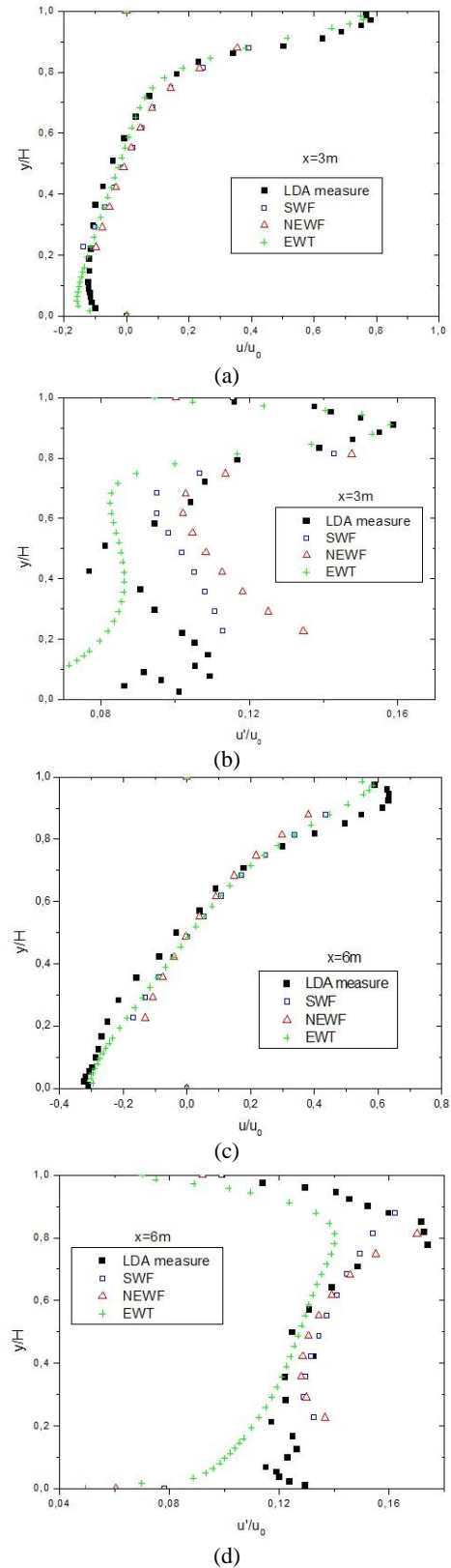


Fig. 9. Comparison between predicted profiles using standard $k-\epsilon$ model with different wall treatments and experimental data for test case 2 benchmark test for a room air distribution. (a) mean velocity at $x=3m$, (b) RMS fluctuation velocity at $x=3m$, (c) mean velocity at $x=6m$, (d) RMS fluctuation velocity at $x=6m$.

At $x=3m$, EWT provides accurate velocity (Fig. 9(a)) and RMS (Fig. 9(b)) for $0.8 < y/H < 1$. However, it under-predicts velocity for $0 < y/H < 0.2$ (Fig. 9(a)). At the opposite, at $x=6m$ velocities obtained by EWT are well predicted for $0 < y/H < 0.2$ (Fig. 9(c)) while they are under-predicted for $0.8 < y/H < 1$. These observations suggest that the flow is well predicted near the inlet and the outlet. At 3m, the flow is well predicted in the upper part (inlet), while at 6m the flow is better described in the lower part (outlet). This could be related to recirculation zones which are not well described in these simulations.

4. CONCLUSIONS

Airflow simulations with different near-wall treatments were applied to two test cases.

The first test case, is the fully developed plane channel flow, similar to a flow through a long corridor in a building, simulation results: i.e. mean stream wise velocity and TKE profiles, were compared to DNS data for $Re_{\tau} = 590$. Standard "SWF" and non equilibrium "NEWF" wall functions need a coarse mesh. The first node should be at $y^+ > 30$. "SWF" and "NEWF" wall functions predict well velocity profiles for $y^+ > 30$ and TKE profiles for $y^+ > 60$. However, they are not able to provide details about velocity and TKE in the viscous and buffer layers. Enhanced wall treatment "EWT" needs a finest mesh in the viscous sublayer. The first node should be at about $y^+ \approx 1$. Velocity profile is more accurate and well predicted even in the viscous and buffer layers. TKE is underestimated; this could provide an underestimated eddy viscosity/diffusivity and therefore could have an effect on predicted temperature and particles concentration. Simulations do not show any difference between standard and RNG $k-\varepsilon$ models. The underestimated TKE seems therefore associated to near wall treatments.

For the second test case, which is a benchmark one for a room air distribution, simulation results for mean velocity and turbulence intensity (at $x/L=1/3$ and $2/3$) were compared to experimental data. No values obtained for all simulations, by wall functions (SWF and NEWF) in the case of $0 < y/H < 0.2$ and $0.8 < y/H < 1$, only "EWT" provides results. This is due to the required mesh and first near wall node. Predicted mean velocity profiles with different near-wall treatments are quite similar for $0.2 < y/H < 0.8$. However, "EWT" provides velocities near the walls where the wall functions are unable to provide values. At $x=3m$ ($x/L=1/3$), all near-wall treatments fail to predict measured RMS velocities u' for $0.2 < y/H < 0.5$. EWT provides accurate velocity and RMS for $0.8 < y/H < 1$. However, it under-predicts velocity for $0 < y/H < 0.2$. At the opposite, for $x=6m$ ($x/L=2/3$), velocities obtained by EWT are well predicted for $0 < y/H < 0.2$ while they are under-predicted for $0.8 < y/H < 1$. These observations suggest that the flow is well predicted in the upper part at $x=3m$ (inlet), while it is better described in the lower part at $x=6m$ (outlet). This seems to be in relation with recirculation zones, which are not well described. More advanced models with adequate near-wall treatments are needed for an efficient simulation of indoor airflow distribution. In our future work, we will access Low Reynolds Number models.

REFERENCES

- Absi R. (2009). A simple eddy viscosity formulation for turbulent boundary layers near smooth walls, *C. R. Mecanique, Elsevier*, 337, 158-165.
- Bahlaoui A., A. Raji, M. Hasnaoui, C. Ouardi, M. Naïmi and T. Makayssi (2011). Height Partition Effect on Combined Mixed Convection and Surface Radiation in a Vented Rectangular Cavity, *Journal of Applied Fluid Dynamics*, 4(1), 89-96.
- Chen H. C. and V. C. Patel (1988). Near-Wall Turbulence Models for Complex Flows Including Separation. *AIAA Journal*, 26(6), 641-648.
- Chen Q (1995). Comparison of Different $k-\varepsilon$ Models for Indoor Air Flow Computations, *Numerical Heat Transfer*, 28, part B, pp 353-369.
- Chen Q. and Z. Jiang (1992). Significant questions in predicting room air motion, *ASHRAE Transactions*, 98(1), 929-939.
- Chen Q. and Z. Jiang (1992). Air supply method and indoor environment, *Indoor environment*, 1, 88-102
- El Gharbi N. (2007). Modélisation et simulation du transfert de chaleur et de masse dans un espace confiné : application au conditionnement d'air d'une salle de chirurgie, mémoire de magistère en physique option Energétique et Mécanique des Fluides, USTHB, Alger.
- El Gharbi N., Benzaoui A., Khalil E.E., Kameel R., (2012). Analysis of indoor air quality in surgical operating rooms using experimental and numerical investigations, *Mechanics & Industry*, 13(2), 123-126.
- Fluent Inc. (2005). *Fluent 6.2 user's guide*.
- Haghighat F, Z. Jiang, J. C. Y. Wang and F. Allard (1992). Air Movement in Buildings Using Computational Fluid Dynamics, *Transactions of the ASME*, 114, 84-92.
- Jongen T. (1992). *Simulation and modeling of turbulent incompressible flows*, PhD thesis, EPF Lausanne, Lausanne, Switzerland.
- Kader B. (1993). Temperature and Concentration Profiles in Fully Turbulent Boundary Layers. *Int. J. Heat Mass Transfer*, 24(9), 1541-1544.
- Kim S.E. and D. Choudhury (1995). A Near-Wall Treatment Using Wall Functions Sensitized to Pressure Gradient, *ASME FED*, 217, Separated and Complex Flows, *ASME*.
- Launder B. E. and D. B. Spalding (1974). The Numerical Computation of Turbulent Flows, *Computer Methods in Applied Mechanics and Engineering*, 3, 269-289.

- Moser R.D., J. Kim, N. N. Mansour (1999). Direct numerical simulation of turbulent channel flow up to $Re\tau = 590$, *Phys. Fluids*, 11(4), 943-500.
- Murakami, S., S. Kato and Y. Suyama (1987). Three-Dimensional Numerical Simulation of Turbulent Airflow in a Ventilated Room by Means of a Two-Equation Model, *ASHRAE Transactions*, 93(2), 621-641.
- Nielsen P. V. (1989). Numerical prediction of air distribution in rooms, *ASHRAE, Building systems: room air and air contaminant distribution*.
- Nielsen P. V. (1990). Specification of a two-dimensional test case, the University of Aalborg, ISSN 0902-7513 R9040.
- Spalding, D. B. (1961). A single formula for the law of the wall, *Trans. ASME., J. Appl. Mech.*, 28, 444-458.
- Sumon S., H. M. Arif, H. Zakir and I. Sadrul (2008), Mixed Convection in an Enclosure with Different Inlet and Exit Configurations, *Journal of Applied Fluid Dynamics*, 1(1), 78-93.
- Weathers, J. W. (1992). *A Study of Computational Fluid Dynamics Applied to Room Airflow*, M S Thesis, Oklahoma State University.
- Wolfstein M. (1969). The Velocity and Temperature Distribution of One-Dimensional Flow with Turbulence Augmentation and Pressure Gradient. *Int. J. Heat Mass Transfer*, 12, 301-318.
- Yakhot V., Orszag, S.A., Thangam S., Gatski T.B., Speziale C.G., (1992). Development of turbulence models for shear flows by a double expansion technique, *Physics of Fluids A*, 4(7), 1510-1520.